Shallow cryogenic treatment: effect on the corrosion resistance and hardness properties of AA5083-H111 alloy in chloride-ions enriched medium

Materials Research Express

PAPER

Shallow cryogenic treatment: effect on the corrosion resistance and hardness properties of AA5083-H111 alloy in chloride-ions enriched medium

Dogancan Uz[1], **Moses M Solomon**[2], **Husnu Gerengi**[1], **Mukerrem Sahin**[3] **and Mesut Yıldız**[1]

[1] Corrosion Research Laboratory, Department of Mechanical Engineering, Faculty of Engineering, Duzce University, 81620 Duzce, Turkey
[2] Department of Chemistry, College of Science and Technology, Covenant University, Canaanland, Km10, Idiroko Road, Ota, Ogun State, Nigeria
[3] Department of Energy Systems Engineering, Faculty of Engineering and Natural Sciences, Ankara Yıldırım Beyazıt University, Ankara, Turkey

E-mail: moses.solomon@covenantuniversity.edu.ng

Keywords: aluminium alloy, cryogenic treatment, cryogenic time, hardness, corrosion resistance, roughness

OPEN ACCESS

RECEIVED
17 June 2021

REVISED
7 July 2021

ACCEPTED FOR PUBLICATION
14 July 2021

PUBLISHED
23 July 2021

Abstract

The influence of cryogenic and cryogenic time (10, 24, 36, 48, and 72 h) on the hardness, surface roughness, and corrosion resistance properties of AA5083-H111 alloy in 3.5 wt.% NaCl solution have been investigated. The hardness property was analysed via the Brinell hardness measurement, the corrosion resistance property was measured electrochemically, while the morphological studies were undertaken using the SEM (scanning electron microscopy) and atomic force microscopy (AFM). The results disclose that the shallow cryogenic treatment at −80°C improves the alloy's hardness, surface roughness, and the corrosion resistance. The best cryogenic treatment time is 24 h. Cryogenic treatment for 24 h increases the alloy's hardness from 71.3 HB to 74.90 HB, reduces the average surface roughness from 534.000 nm to 105.634 nm, and increases the total charge transfer resistance from 18139 Ω cm^2 to 26230 Ω cm^2. The improvement is linked to settling of fine particles on the alloy surface. The SEM results support these claims.

1. Introduction

There is a fast-growing trend on the use of aluminium-alloys in shipbuilding and other marine services [1] due to features such as low weight, good dissolution resistance, and good mechanical properties [1, 2]. The 5083 and 6082 Al-alloy series, which are the most used Al-alloys in maritime industry [1, 2], exhibit yield strength requirements equivalent to that of steels [1] in addition better corrosion and mechanical properties relative to other grades [2].

The process of gradual cooling of a sample from room temperature to extremely low temperature and to room temperature again is referred as to cryogenic treatment [3–6]. The sample is allowed to stay at the extreme temperature for a long duration and then gradually, it is brought back to normal temperature [3–6]. During this process, the sample shrinks causing the sample's atoms to be rigidly held together [7]. The process could be termed shallow and deep depending on the temperature at which it is carried out [3]. For shallow cryogenic treatment, the sample is frozen to about −80°C [2, 8, 9] whereas, in deep cryogenic treatment, the sample is cooled to temperature as low as −196 °C [5, 6, 10, 11]. It had been reported that, cryogenic treatment improves material properties and durability [2, 3, 7]. Pan *et al* [11] conducted experiments to ascertain the contributions of deep cryogenic treatment to the microstructure and deterioration behaviour of a microarc oxidized Mg-2.0Zn-0.5Ca alloy. The process was found to have a refining influence on the microstructure and the grain size of the alloy; induced phase condensation and as well created crystal defect states in the examined alloy. Haramritpal *et al* [10] investigated the extent to which subjecting a Friction Stir Processed (FSPed) magnesium alloy to cryogenic process will have on the mechanical property and on the corrosion characteristics in sodium chloride solution. The corrosion resistance and mechanical property of the cryogenically treated magnesium alloy

Table 1. Weight percentage composition of AA5083-H111 alloy.

AA5083-H111	Si	Fe	Cu	Mn	Mg	Cr	Zn	Ni	Ti	Sn	Zr	Al
	0.075	0.404	0.031	0.276	4.300	0.081	0.012	0.007	0.018	<0.002	<0.005	94.796

samples were found to improve remarkably relative to that of the control. The improvement was associated with the scattering of particles with deep cryogenic treatment. Uygur *et al* [2] reported improved dissolution resistance characteristic for AISI D3 steel in chloride-enriched solution occasioned by cryogenic treatment. Baldissera and Delprete [6] reported an enhanced fatigue property and no effect on hardness property of solubilized AISI 302 after deep cryogenic practice. Similarly, cryogenic practices have been found to be beneficial in protecting magnesium alloys against stress corrosion cracking in simulated body fluid [12].

The debate on which cryogenic treatment method is better, shallow or deep and the influence of cryogenic time on the process is ongoing. Senthilkumar *et al* [8], in their comparative studies on the effect of the two types of cryogenic practices on the residual stress state of 4140 steel claimed that shallow process encouraged tensile state of residual stress while the deep process showed a compressive residual stress. Arunram *et al* [9] reported improvement in the hardness property of steel grade M2 drilling tool by 40.96% through deep cryogenic treatment for 30 h and an increase of 31% in hardness by shallow cryogenic treatment for 30 h. Sonar *et al* [3], in their review advocated for deep cryogenic treatment of materials and a soaking period of 24 h in expense of shallow treatment process. However, in the investigation of Gao *et al* [5] on the contributions of cryogenic duration (2 h, 12 h and 24 h) to microstructure, mechanical, and dissolution resistance properties of WC–Fe–Ni cemented carbides noted that, during deep cryogenic treatment at –196°C, the corrosion resistance property of the cemented carbides diminished. The study revealed that, prolonging treatment duration ensured phase conversion, which in turn improved the studied properties.

As part of our contribution to this area of research, this work is designed to examine the effect of shallow cryogenic treatment (–80°C) and cryogenic time (10 h, 24 h, 36 h, 48 h, and 72 h) on the hardness, surface roughness, and corrosion resistance properties of AA5083-H111 alloy in a chloride-enriched system. The hardness property of the alloy before and after cryogenic treatments is analysed by Brinell hardness measurement. The corrosion resistance property is realized by studying the electrochemical behaviour of the alloy and the morphological changes on the alloy surface before and after exposure to studied medium. The electrochemical impedance spectroscopy (EIS) technique is used for electrochemical studies while the SEM and AFM techniques are used for morphological studies.

2. Material, chemical, and experimental procedures

2.1. Material and chemical preparation

The material considered in this study is AA5083-H111 alloy metal. It was procured from ALRO SA, Romania and in table 1 is listed the weight percentage content. The alloy with a wall thickness of 6 mm was mechanically cut into rectangular shape (20 mm × 40 mm). The samples for corrosion studies were encapsulated to expose only 0.785 cm^2 as the working area. The corrosion medium was 3.5 wt.% NaCl solution prepared by dissolving appropriate amount of NaCl salt (Sigma-Aldrich) in distilled water.

2.2. Cryogenic treatment of samples

Prior to the cryogenic treatment process, the AA5083-H111 alloy samples were mechanically abraded using various grits (400, 600, 800, and 2000) of abrasion papers. Thereafter, the samples were washed in distilled water and acetone so as to remove the dusts generated from the abrasion process and finally dried in warm air (about 40°C). The prepared samples were subjected to shallow cryogenic treatment by placing the samples in a Core DF 490 device and slowly cooling from room temperature to −80°C. The samples were soaked at −80°C for different durations (10 h, 24 h, 36 h, 48 h, and 72 h) in order to ascertain the influence of cryogenic time on studied properties. At the end of the specified time, the samples were kept at room temperature for 2 h before measurements.

2.3. Brinell hardness measurement

The hardness property of AA5083-H111 alloy samples un-cryogenically and cryogenically treated were measured using a DIGIROCK-RB hardness tester. A load of 100 kg was applied on each sample with the help of an 1/18 inch diameter ball system and with a dwell period of 5 sec. Each experiment was repeated for seven times and the average value is presented in this work.

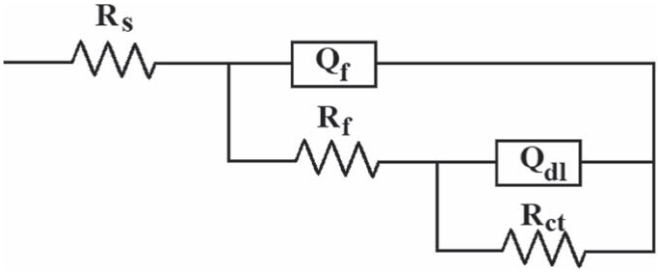

Figure 1. Equivalent circuit used for the analysis of electrochemical impedance data. R_s is the solution resistance, R_f is the film resistance, R_{ct} is the charge transfer resistance, and Q is the constant phase element (CPE).

2.4. Corrosion resistance measurement

2.4.1. EIS experiments

The dissolution resistance property of AA5083-H111 samples un-cryogenically and cryogenically treated in the chloride-enriched solution were studied using the EIS technique. Experiments were performed on a Gamry Reference 600 potentiostat/galvanostat/ZRA instrument. The experimental setup consisted of the AA5083-H111 sample as the working electrode, a platinum rod as the counter electrode, and a Ag/AgCl reference electrode. Before each electrochemical measurement, the working electrode was trapped in test solution for 21600 s. Impedance measurements were done at the frequency range of 0.1 Hz to 100000 Hz and amplitude of 10 mV peak to peak. All electrochemical corrosion studies were carried out at room temperature and each experiment was repeated for seven times under same conditions to ensure reproducibility. The impedance analysis was made with the help of a ZsimpWin 3.21 software and the selected equivalent circuit is shown in figure1.

2.4.2. Surface analysis experiments

After the EIS experiments were performed on AA5083-H111 alloy samples, the samples surfaces were examined using SEM, energy dispersive x-ray spectroscopy (EDX), and AFM. The SEM and EDX analysis were performed using a J. Quanta FEG 250 (FEI, Holland) model device. The instrument was accelerated at 10 kV. The AFM analysis was achieved with PARKSYSTEMS, XE-100E model (UK) instrument.

3. Results and discussion

3.1. Analysis of surface corrosion products

The AA5083-H111 alloy contains magnesium as the major alloying element and several other elements (table 1). The presence of these alloying elements give rise to second phase particles (Al_6Mn, Al_6MnFe, Mg_2Si, Al_3Mg_2, Al-Si, Al-Mn, Al-Fe, Al-Cr, etc.) formation within the metal composite parts and along the interface between grains [13] which the variance in the electrochemical potential of the matrix and the second phases makes Al alloys to be prone to corrosion of different forms including the localized pitting corrosion [14–16]. For the AA5083 alloy grade, two parallel corrosion processes are proposed [13, 17]. Firstly, corrosion is based on the cathodic stimulation of the Al part by the rapidly anodic dislodging of Fe-rich intermetallic particles like Al_6MnFe, Al-Fe, etc. [13, 17]. Secondly, it is based on the chemical and electrochemical activities of Mg_2Si, that often result in the selective leaching of Mg and the precipitation of $SiO_2{\cdot}nH_2O$ and/or magnesium hydroxide [17].

Figure 2 depicts the SEM micrographs of the as-received AA5083-H111 alloy at (a) 2000 magnification and (c) 10,000 magnification after exposing to the studied chloride-rich medium at 25°C for 24 h. The associated EDX spectra are shown in figures 2(b) and (d), respectively. The elemental mapping of the corroded surface is shown in figure 2(e). Obviously, the alloy surface corroded severely in the chloride-rich solution. In figure 2(a), a severely damaged surface with different sizes of pits is seen. Similar localized pitting corrosion was reported by Beura *et al* [13] for dynamically deformed Al–Mg (AA5083) alloy in 0.6 M NaCl solution. It is believed that defects on aluminium matrix are responsible for the growth of oxide layers that serve as the initiation sites for chloride ion absorption in a chloride-rich medium [14–16]. The Point defect model [18, 19] stipulates that the initiation of pitting corrosion in Al alloys is the attachment of Cl^- ions on anion vacancies of oxide layer. The inspection of the EDX spectrum in figure 2(b) reveals that the alloy surface is rich in chlorides and oxides. The adsorption of the chloride ions on the oxide layer may have shrinks the corrosion resistance property of the alloy [16]. It is also true from figures 2(c)–(e) that the Al-Fe and Al-Mn second phases contributed significantly to the corrosion of the alloy in the studied medium. As could be seen in figures 2(d) & (e), Fe and Mn are the major

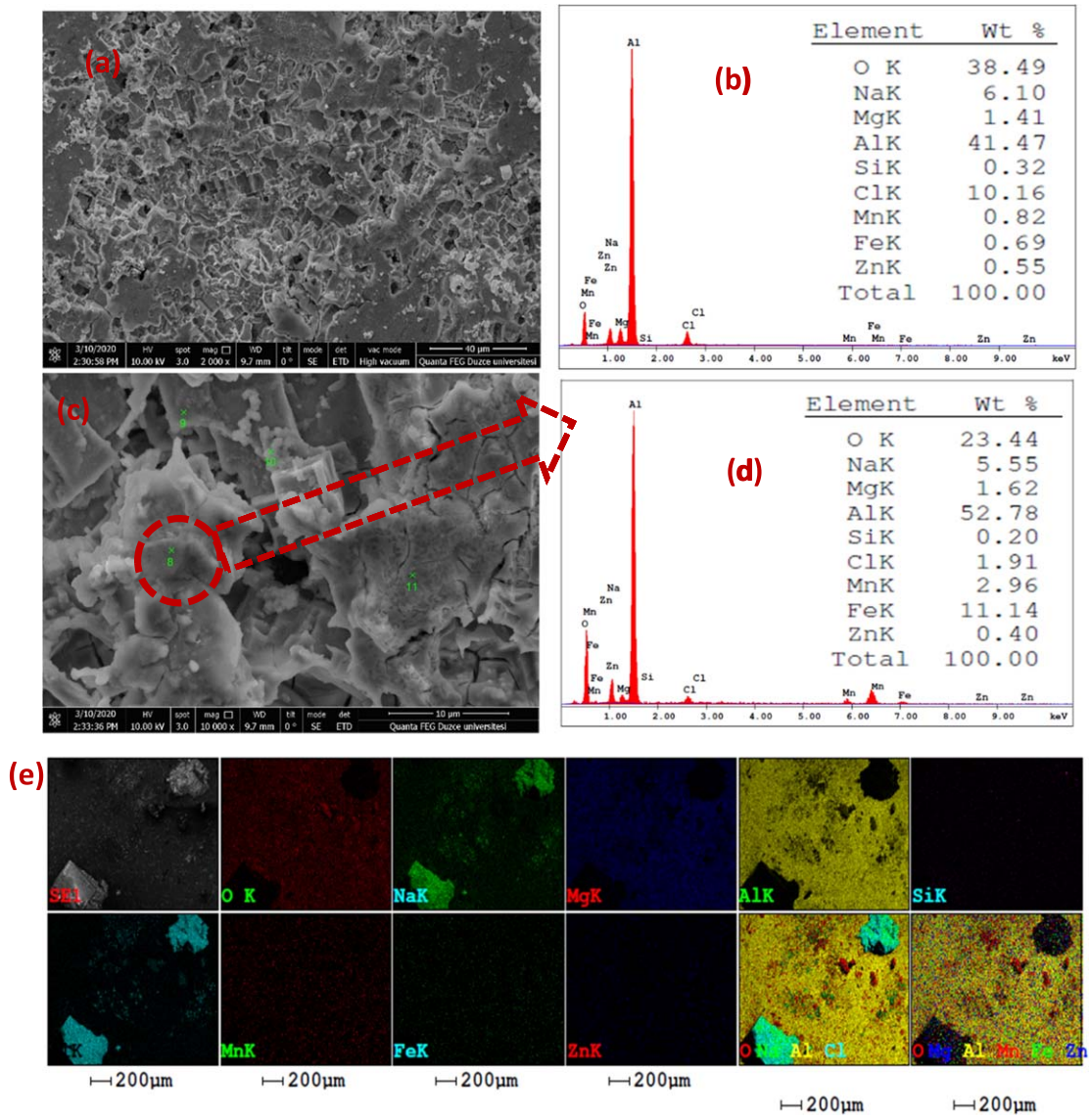

Figure 2. SEM micrographs of un-cryogenic treated AA5083-H111 alloy at (a) 2000 magnification and (c) 10,000 magnification after immersion in 3.5 wt.% NaCl solution at 25°C. The corresponding EDAX spectra are given in (b) and (d), respectively. The elemental mapping of the corroded surface is shown in (e).

components of the corrosion products conforming with the report of others [13, 17] that AA5083 alloy grades corrode mostly along these second phase particles.

Figure 3 depicts the SEM micrographs of 10 h cryogenically treated AA5083-H111 alloy at (a) 2000 magnification and (c) 10,000 magnification after exposure to studied medium at 25°C. Figures 3(b) & (d) present the corresponding EDX spectra while the elemental mapping of the corroded surface is shown in figure 3(e). Generally, the idea of metals cryogenic treatment is based on two main reasons: (a) to eliminate retained austenite [2, 12] and (b), to initiate nucleation sites for the condensation of fine particles [2, 12]. It is also believed that cryogenic treatment slows down atomic level movements within a metal system, which in turn diminishes the system energy causing the metal to be chemically less reactive to its environment [3]. It is obvious that the pitting corrosion observed in figure 2(a) is reduced in figure 3(a). The surface in figure 3(a) is rather covered with products, which the EDX spectra in figures 3(b) & (d) reveal are different from the deposits found on the surface of the un-treated alloy (figure 2(a)). The product is enriched in Na (figures 3(b) & (d)). It could be the precipitated particles that decreased the surface area for the ingression of chloride ions into the metal. Uygur *et al* [2] had reported the improvement of the deterioration resistance property of AISI D3 steel in sodium chloride solution after shallow cryogenic treatment occasioned by the precipitation of secondary fine particles. Ramesh *et al* [20] documented that deep cryogenic practice encouraged the settling of secondary fine particles on structural steel samples and this enhanced the corrosion resistance of the steel. It however, appears from figures 3(a) & (e) that the precipitated products did not cover the entire surface. In fact, by closing inspecting

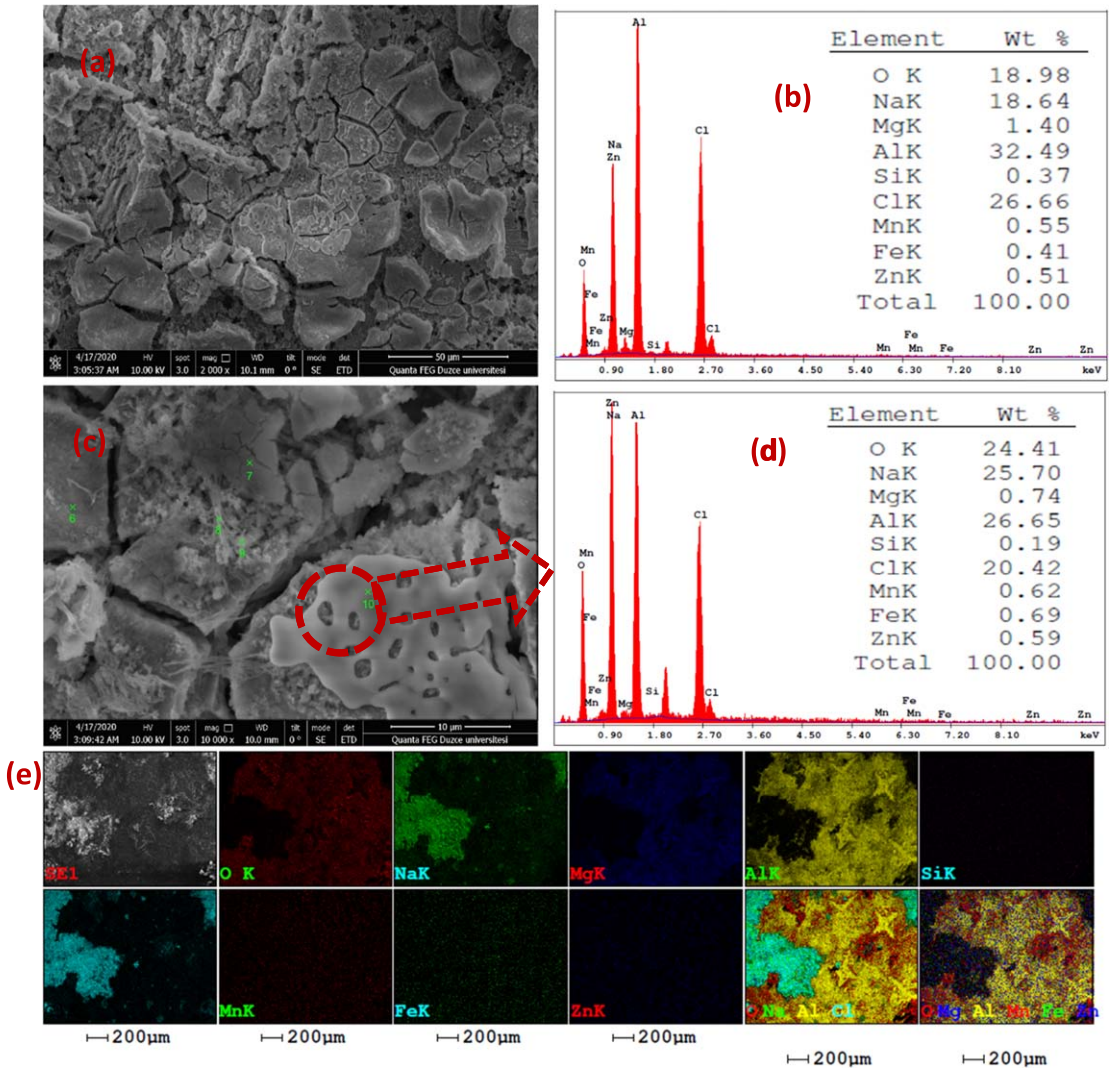

Figure 3. SEM micrographs of 10 h cryogenically treated AA5083-H111 alloy at (a) 2000 magnification and (c) 10,000 magnification after immersion in 3.5 wt.% NaCl solution at 25°C. The corresponding EDAX spectra are given in (b) and (d), respectively. The elemental mapping of the corroded surface is shown in (e).

figure 3(a), one could still see some pits on the surface. The rate of precipitation of the products and its distribution may have a lot to do with cryogenic treatment time. Although there is no definite procedure provided in the cryogenic literature for the selection of soaking period for materials, authors have continued to lay emphasis on sufficient soaking time. According to Sonar *et al* [3], at least 24 h soaking time at cryogenic temperature is required. Paulin [21] opined that a long soaking time is essential for the complete conversion of left on austenite into martensite and condensation of fine particles.

The surfaces subjected to cryogenic treatment for 24–72 h are shown in figures 4(a)–(d) and the corresponding EDX images are presented in (e-h). The influence of cryogenic time on the precipitated particles is evident in the SEM micrographs (figures 4(a)–(d)). Denser, more rigid and more coherent products are seen on the surfaces compared to the surfaces in figures 2 and 3. Consequently, less pitting is seen on the surfaces in figures 4(a)–(d) relative to the surfaces in figures 2(a) and 3(a). Worthy of pointing out is the uniform distribution of the particles subjected to 24 h of cryogenic treatment (figure 4(a)) and the rougher morphology of the surface exposed to 72 h of cryogenic treatment (figure 4(d)) relative to others. These observations could have effect on the properties of the surfaces. The EDX results (figures 4(e)–(h)) reveal that the precipitates are rich in oxides but low in chlorides. It had been postulated that cryogenic treatment induced nano-sized grains precipitation and the grains promote the formation of passive oxide films that enhance surface corrosion resistance property [10, 20, 22, 23]. More so, compared to the EDX spectrum in figures 2(b) & (d), the composition of Al and Mg in figures 4(e)–(h) significantly increased. Recently, Syed *et al* [23] identified $Al_xFe_xSi_x$ and Mg_2Si as the precipitates on Al 6101 foam after cryogenic treatment.

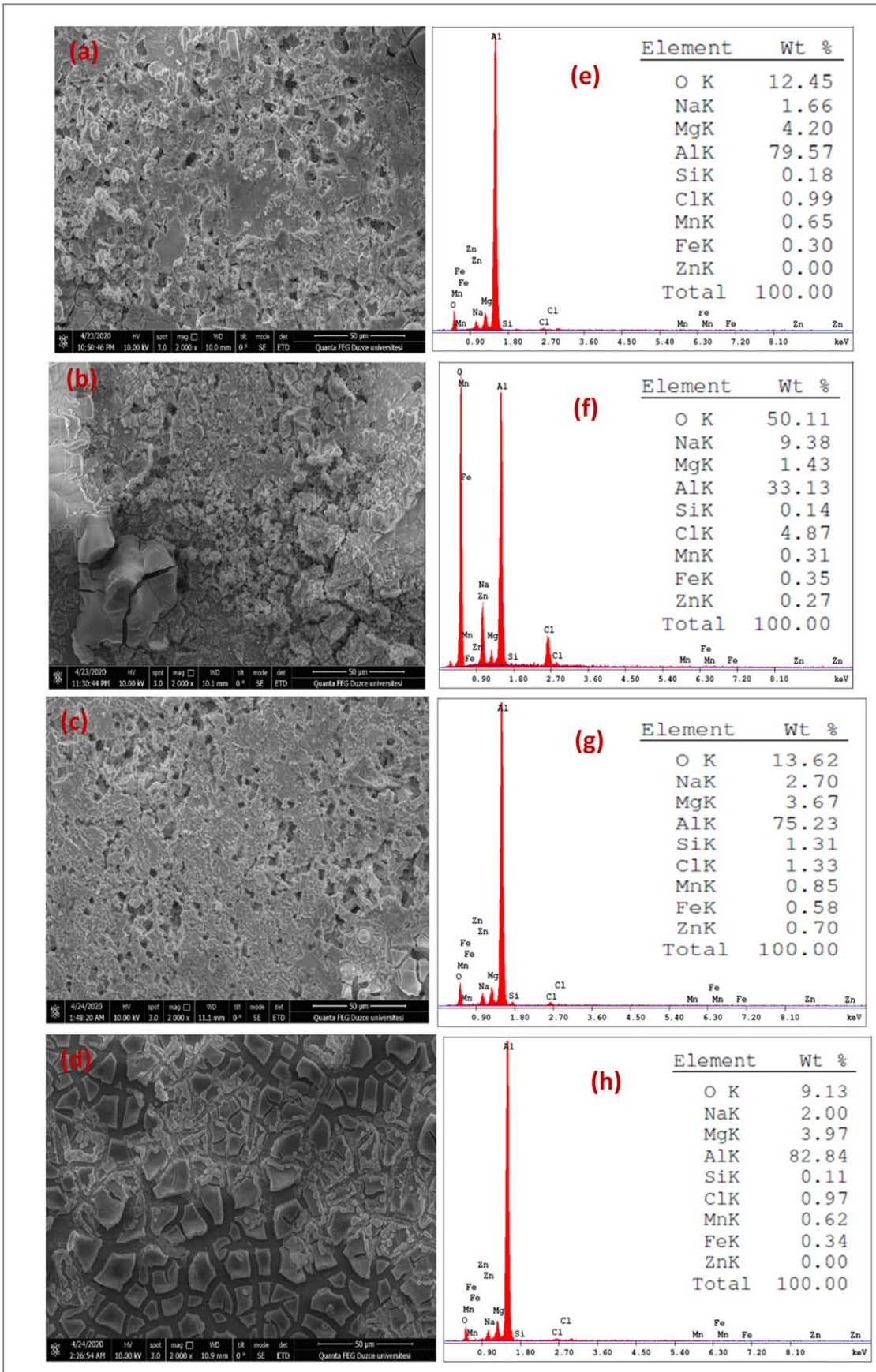

Figure 4 SEM micrographs of (a) 24 h, (b) 36 h, (c) 48 h, and (d) 72 h cryogenically treated AA5083-H111 alloy at after immersion in 3.5 wt.% NaCl solution at 25°C. The corresponding EDX spectra are shown in (e)–(h).

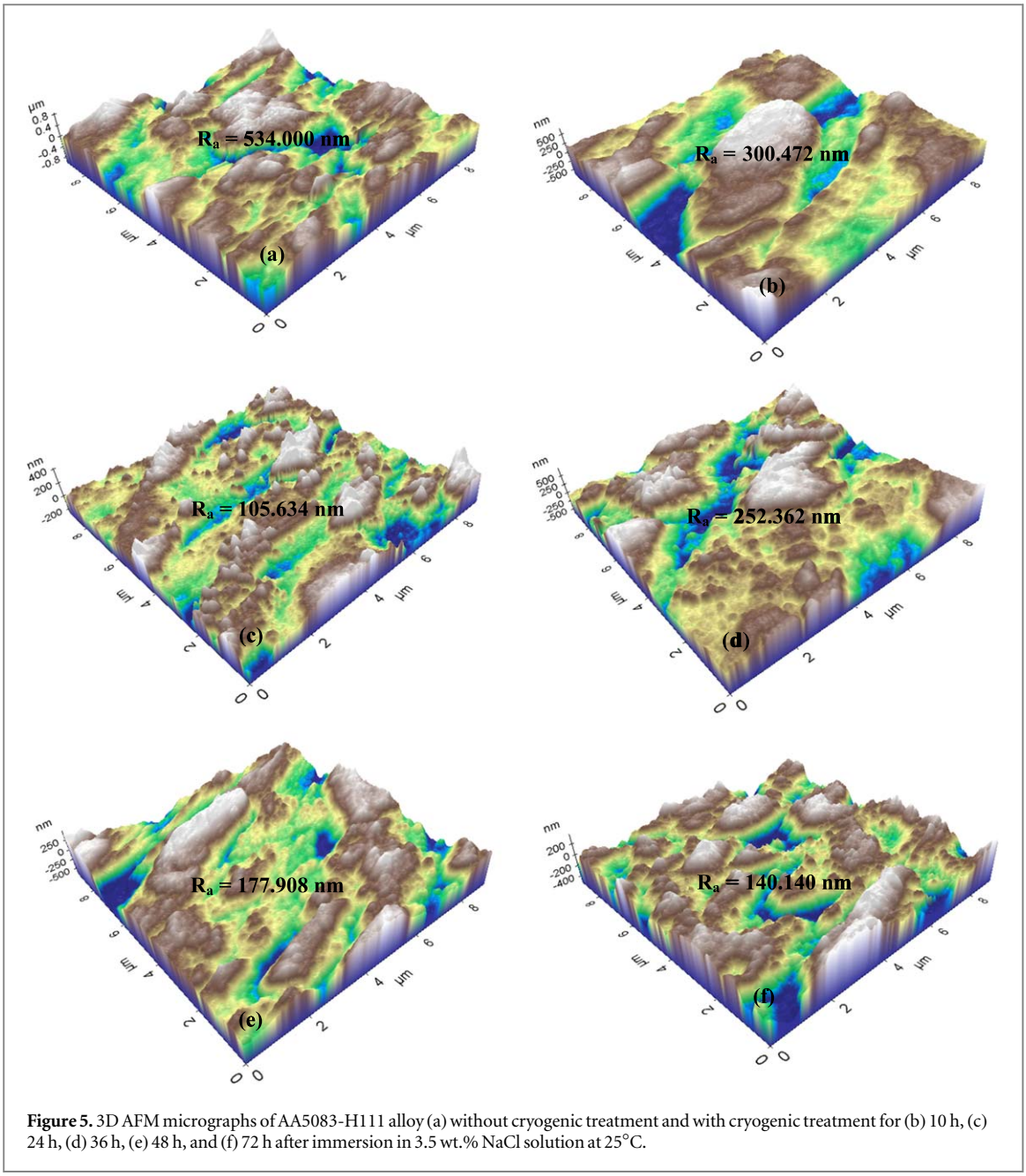

Figure 5. 3D AFM micrographs of AA5083-H111 alloy (a) without cryogenic treatment and with cryogenic treatment for (b) 10 h, (c) 24 h, (d) 36 h, (e) 48 h, and (f) 72 h after immersion in 3.5 wt.% NaCl solution at 25°C.

3.2. Analysis of surface roughness

Figure 5 displays the 3D AFM images of AA5083-H111 alloy (a) without cryogenic treatment and with cryogenic treatment for (b) 10 h, (c) 24 h, (d) 36 h, (e) 48 h, and (f) 72 h after exposing to studied medium at 25°C. The average roughness (R_a) value is inserted in the micrographs. A comparison of the surfaces in figures 5(b)–(f) with figure 5(a) reveals smoother surface topography in figures 5(b)–(f) than in figure 5(a). This observation which is in conformity with previous reports [20, 24, 25] indicates least vulnerability of the treated surfaces to corrosion attack [20]. According to Ramesh *et al* [20], the rougher topography of the untreated surface translates to higher corrosion susceptibility and is due to the absence of precipitates.

The R_a value is very valuable when it comes to checking the quality of a material surface [25]. Generally, the smaller the R_a value, the higher the surface quality. A surface with considerable small value of R_a is deemed to have lesser defects and free from adhesion of foreign particles [20, 25]. It is also believed that homogeneity of a surface can limit surface corrosion attack [20, 25]. In this work, R_a value for the untreated AA5083-H111 alloy after corrosion in NaCl solution is 534.000 nm. The value is reduced to 300.472 nm, 285.634 nm, 105.362 nm, 177.908 nm, and 140.140 nm on surfaces cryogenically treated for 10 h, 24 h, 36 h, 48 h, and 72 h, respectively. This corresponds to reduction by 43.73%, 80.21%, 52.74%, 66.68%, and 73.76%, respectively. Similar significant reduction in R_a value after cryogenic treatment was observed by Agrawal *et al* [25] and was interpreted to mean improvement of surface properties. Based on the R_a value, 24 h is the best cryogenic treatment time. It is

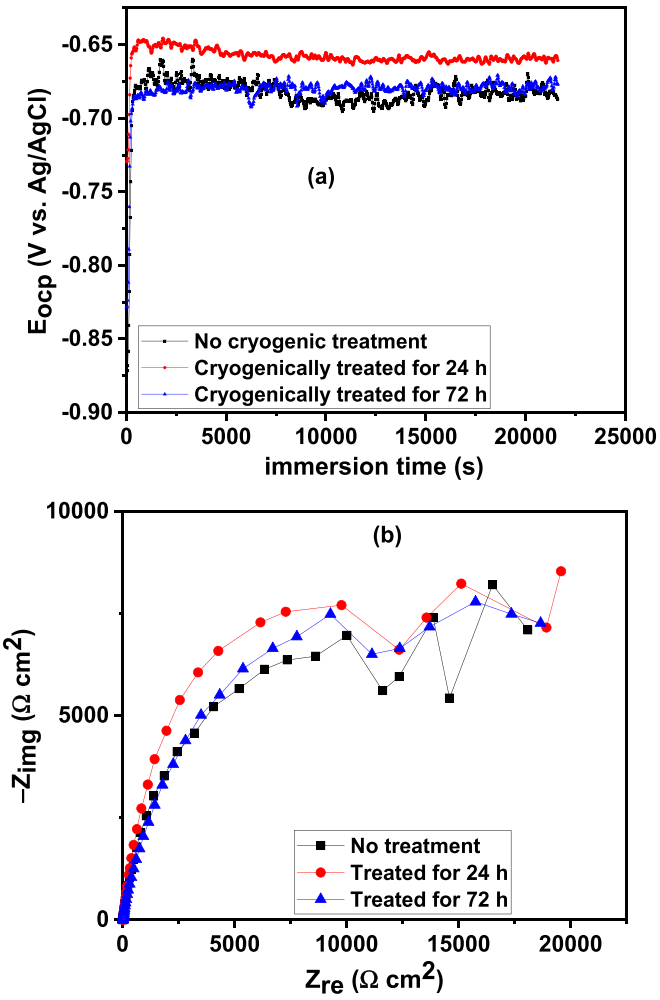

Figure 6. (a) Open circuit potential versus time and (b) impedance plots for AA5083-H111 alloy without and with cryogenic treatment in 3.5 wt.% NaCl solution at 25°C.

in conformity with the report of Özbek *et al* [26]. The authors had examined the role of cryogenic practice at various retention times (12 h, 24 h, 36 h, 48 h and 60 h) on cemented carbide inserts on tool wear and found best wear resistance for 24 h cryogenically treated samples. Again, the observation was attributed to better improvement of surface properties of the cemented carbide inserts at 24 h of treatment.

3.3. Analysis of corrosion resistance

To acquire insight into the effect of cryogenic treatment on the dissolution resistance property of AA5083-H111 alloy in the studied environment, the Open-Circuit Potential (E_{ocp}) of the as-received, 24 h, and 72 h cryogenically treated AA5083-H111 alloy samples was monitored at 25°C for 21600 s. The results obtained are presented in figure 6(a). Both the as-received and the treated alloy samples behave alike at the beginning of the experiments. The E_{ocp} of the as-received, 24 h, and 72 h cryogenically treated samples begins at −0.87 V versus Ag/AgCl, −0.73 V versus Ag/AgCl, and −0.83 mV versus Ag/AgCl, respectively and progresses anodically for about 2500 s before flattering (figure 6(a)). Such progression, which had been reported by others [27–29] is due to the premier deterioration of the pre-exposed, air-formed oxide layer, and the attack on the alloy samples surfaces [27–29]. Compared to the E_{ocp} of the as-received, the E_{ocp} of the cryogenically treated samples is displayed toward nobler potentials indicating higher resistance of the treated samples to corrosion processes [27]. It means that the cryogenic treatment improves the corrosion resistance property of the alloy. By comparing the E_{ocp} of the 24 h and 72 h treated samples, the 24 h treated sample is found to exhibit nobler potential than the 72 h treated sample. For instance, the E_{ocp} at 21600 s for the 24 h treated sample is −0.66 V versus Ag/AgCl while that of the 72 h treated sample is −0.68 V versus Ag/AgCl. This points to superior resistance to corrosion by the 24 h cryogenic treated sample than the 72 h treated sample. These results are in consonance with the AFM results (figure 5).

Table 2. EIS parameters obtained during corrosion of AA5083-H111 alloy un-cryogenically and cryogenically treated for 24 h and 72 h in 3.5 wt.% NaCl solution at 25°C.

	R_s	CPE_{dl}		R_{ct}	CPE_f		R_f	($R_p = R_f + R_{ct}$)	Improvement(%)
State of alloy	(Ω cm^2)	Y_{dl} (μF cm^{-2} s^{n-1})	n_{dl}	(Ω cm^2)	Y_f (μF cm^{-2} s^{n-1})	n_f	(Ω cm^2)	(Ω cm^2)	
Untreated	8.7	17.2	0.91	10,700	366.0	0.99	7,439	18,139	—
Treated-24 h	9.0	13.5	0.90	13,070	211.0	0.98	13,160	26,230	30.85
Treated-72 h	9.7	15.6	0.89	10,717	230.0	0.92	8,474	19,191	5.48

At the end of the open circuit potential experiments, the impedance characteristics of the alloy samples were collected. Figure 6(b) shows the impedance spectra of AA5083-H111 alloy without and with cryogenic treatment in the studied medium at 25°C. Depressed semicircles are observed in all cases and is a characteristic of a metallic electrode whereby dissolution process is driven by a charge transfer [27, 30]. The capacitive loops in both the as-received and cryogenically treated samples are same and indicates same mechanism of corrosion [27]. However, the treated samples exhibit bigger capacitive loops relative to the as-received indicating higher corrosion resistance [27, 31, 32]. Again, the capacitive loop of the 24 h treated alloy sample is wider than that of the 72 h treated sample agreeing with other results (figures 5; 6(a)) that the best cryogenic treatment time for the studied substrate is 24 h. The values of the solution resistance (R_s), the components of constant phase element (Y_0 and n), the charge transfer resistance (R_{ct}), and the resistance of the surface film (R_f) obtained from the analysis of the impedance data using the equivalent circuit given in figure 1 are summarized in table 2. The total charge transfer resistance, R_p (i.e $R_{ct} + R_f$) of the as-received, 24 h, and 72 h cryogenically treated AA5083-H111 alloy samples is 18139 Ω cm^2, 26230 Ω cm^2, and 19191 Ω cm^2, respectively. This translates to corrosion resistance enhancement of 30.85% and 5.48%, respectively by cryogenic treatment for 24 h and 72 h, respectively. Although cryogenic treatment cannot be recommended as a first choice corrosion control measure in expense of other techniques like surface coatings, it should be mentioned that the beauty of cryogenic technique lies on the fact that corrosion control can be achieved without the metal losing its mechanical and other desired properties [3, 20, 33]. Ramesh *et al* [20] suggested the use of cryogenic treatment on metals meant for special applications like aerospace, freeze-thaw region, etc. The value of Y_0 provides information on the characteristics of a surface film [34]. A small value of Y_0 points to good features of a surface film [34]. The Y_0 values in table 2 reveals better surface film characteristics for the 24 h cryogenically treated surface than the untreated and 72 h treated surfaces. Also worthy of pointing out from table 2 is the fact that both n1 and n2 values for all the surfaces are near unity and this is reflective of capacitive surfaces [35].

3.4. Analysis of hardness

Numerous works have highlighted the positive effect of cryogenic treatment on hardness property of metals. Arunram *et al* [9] reported 16.59% and 25.21% improvement in the hardness of high-speed steel grade M2 drilling tool after shallow and deep cryogenic treatment for 24 h. Amini *et al* [36] observed 4.6% increase in hardness of 80CrMo125 tool steel after deep cryogenic treatment. Similarly, Harish *et al* [37] noted 14% and 13% improvement in the hardness of EN31 bearing steel after deep and shallow cryogenic treatments, respectively. In all these reports, the improvement in hardness property was linked to a reason earlier mentioned - the conversion of hold on austenite to another form (martensite) and the settling of fine secondary particles [9, 36, 37]. Figure 7 presents the variation of the hardness of AA5083-H111 alloy with cryogenic treatment time. It is obvious from the figure that the shallow cryogenic treatment improves the hardness of the alloy. The cryogenic treatment for 10 h, 24 h, 36 h, 48 h, and 72 h increased the hardness of AA5083-H111 alloy from 71.3 HB to 72.43 HB, 74.90 HB, 74.09 HB, 73.83 HB, and 74.57 HB, respectively. The percentage increment is 1.56%, 4.81%, 3.76%, 3.42%, and 4.39%, respectively. The 24 h treatment duration produced the best enhancement on the hardness property (4.81%) in agreement with other experimental results (figures 5 & 6).

3.5. Possible mechanism for the observed improved corrosion resistance and hardness

Cryogenic treatment influences the microstructure of a material in three ways: (i) transformation of retained austenite into martensite, (ii) precipitation of finely dispersed particles, and (iii) relaxation of residual stresses [10, 20]. In most cases, the second effect, that is, precipitation of finely dispersed particles is responsible for the improvement in corrosion resistance property after cryogenic treatment [22, 23]. The fine precipitates are formed in the outer wall microstructures and can interact with dislocations, resist dislocation motion [23], and form Guinier-Preston (GP) zone [38]. The GP zone can ensure enhancement of materials properties. Franco

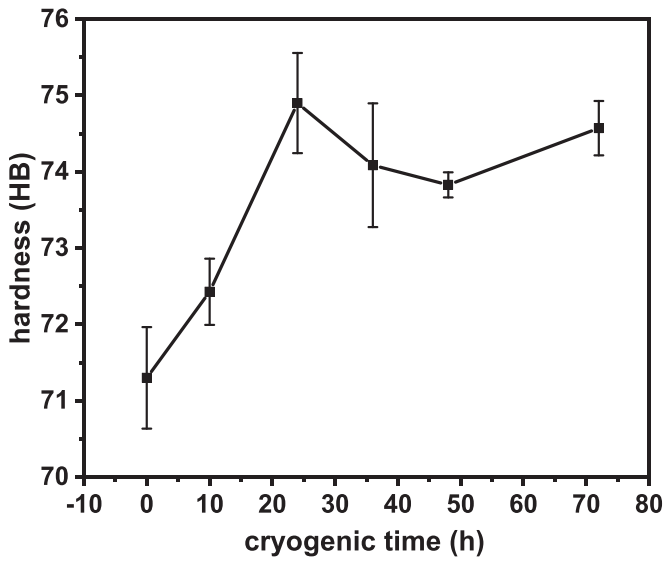

Figure 7. Plots of hardness against cryogenic treatment duration.

Steier *et al* [39] attributed the reduction of wear rates of specimens to the generation of GP zone in the cryogenically treated specimen. Syed *et al* [23] observed that the formation of this zone led to the improvement of hardness property of Al 6101 closed-cell foam after cryogenic treatment. The observed increase in the hardness property of the studied AA5083-H111 alloy could as well be attributed to the action of the precipitated particles.

For the improvement of corrosion resistance property, precipitated particles depending on the volume, type, size, distribution pattern, and shape, can restrict the penetration of corrosive species and in turn decrease the rate of corrosion [22]. Recently, it was reported [23] that $Al_xFe_xSi_x$ and Mg_2Si are the main components of the precipitates on a cryogenically treated 6101 aluminium alloy exposed to 3.5 wt.% NaCl solution. As earlier mentioned, the studied AA5083-H111 alloy contains alloying elements (table 1) that give rise to second phase particles (Al_6Mn, Al_6MnFe, Mg_2Si, Al_3Mg_2, Al-Si, Al-Mn, Al-Fe, Al-Cr, *etc*). Our EDX results (figures 4(e)–(h)) reveal a significant increase in the percentage composition of Al and Mg on the precipitated particles on the cryogenically treated samples surfaces compared to the untreated sample surface (figures 2(b) & (d)). The precipitation of this particles is the reason for the observed corrosion resistance enhancement. Additionally, nano-sized grains that are uniformly distributed can induced the formation of a passive oxide film and this will render the metal surface more electrochemically stable [10, 20, 22, 23]. The less surface roughness of the cryogenically treated surfaces also contributes to the improved corrosion resistance of the alloy. The reduction in surface roughness strengthens the resistance of the surface to corrosive attacks.

4. Conclusions

Cryogenic process involves the gradual freezing of specimen to extreme low temperature, retention at that temperature for as long as 24 h, and reversal to room temperature [3–6]. It has been demonstrated that cryogenic treatment improves certain properties of material [3–6]. In this work, AA5083-H111 alloy samples were subjected to shallow cryogenic treatment at $-80^{\circ}C$ for 10, 24, 36, 48, and 72 h. The effect of the process on the hardness and surface roughness properties of the alloy as well as on the corrosion behaviour of the alloy in 3.5 wt. % NaCl solution was studied. The following deductions are made.

1) The shallow cryogenic treatment improves the hardness, surface roughness, and corrosion resistance properties of AA5083-H111 alloy.
2) The best shallow cryogenic treatment time for the alloy is 24 h.
3) The cryogenic treatment of AA5083-H111 alloy for 24 h increases the hardness property by 4.81%, reduces surface roughness by 80.21%, and improves corrosion resistance by 30.85%.
4) The SEM results confirm the settling of fine particles on the surfaces of the alloys samples in agreement with the results of Syed *et al* [23] that $Al_xFe_xSi_x$ and Mg_2Si precipitates settled on the surface of a cryogenically

treated 6101 aluminium alloy after immersion in 3.5 wt.% NaCl solution and improved corrosion resistance property.

Data availability statement

The data that support the findings of this study are available upon reasonable request from the authors.

Funding

We acknowledge the financial assistance by the Duzce University Research Fund under the Project No: 2020.06.05.1111. The authors express their sincere gratitude to Prof. Dr İlyas Uygur for aiding in the supply of AA5083-H111 alloys.

Conflict of interest

The authors declare that they have no known competing financial interests or personal relationships that could have appeared to influence the work reported in this paper.

Data availability statement

The data that support the findings of this study are available upon request from the authors.

ORCID iDs

Moses M Solomon https://orcid.org/0000-0002-3251-8846
Husnu Gerengi https://orcid.org/0000-0002-9663-4264

References

[1] Pepe N and Quintino L 2006 Metallurgical and corrosion features of friction stir welding of AAS083-H111 *Weld. World* **50** 55–64
[2] Uygur I, Gerengi H, Arslan Y and Kurtay M 2015 The effects of cryogenic treatment on the corrosion of AISI D3 Steel *Mater. Res.* **18** 569–74
[3] Sonar T, Lomte S and Gogte C 2018 Cryogenic treatment of metal-a review *Mater. Today Proc.* **5** 25219–28
[4] Cabibbo M, Santecchia E, Mengucci P, Bellezze T and Viceré A 2018 The role of cryogenic dipping prior to ECAP in the microstructure , secondary-phase precipitation , mechanical properties and corrosion resistance of AA6012 (Al-Mg-Si-Pb) *Mater. Sci. Eng. A* **716** 107–19
[5] Gao Y, Luo B, Bai Z, Zhu B and Ouyang S 2016 Effects of deep cryogenic treatment on the microstructure and properties of WC-Fe–Ni cemented carbides *Int. J. Refract. Met. Hard Mater* **58** 42–50
[6] Baldissera P and Delprete C 2010 Deep cryogenic treatment of AISI 302 stainless steel : part II-fatigue and corrosion *Mater. Des.* **31** 4731–7
[7] Kumar R P and Arul S 2020 Improving the wear and corrosion resistance of nickel aluminium bronze by deep cryogenic treatment *Mater. Today Proc.* (In Press) (https://doi.org/10.1016/j.matpr.2020.10.334)
[8] Senthilkumar D, Rajendran I, Pellizzari M and Siiriainen J 2011 Influence of shallow and deep cryogenic treatment on the residual state of stress of 4140 steel *J. Mater. Process. Tech.* **211** 396–401
[9] Arunram S P, Nishal M, Thirumugham M and Raghunath A G 2020 Effect of deep and shallow cryogenic treatment on high speed steel grade M_2 drilling tool *Mater. Today Proc.* 2–6
[10] Sidhu H S and Singh P K B 2021 Effect of cryogenic treatment on corrosion behavior of friction stir processed magnesium alloy AZ91 *Mater. Today Proc.* (In Press) (https://doi.org/10.1016/j.matpr.2020.12.666)
[11] Pan Y, Wang J, Cui H, Feng R, Gong B, Zhao X, Hou N, Cui B, Song Y and Yang T 2020 Effect of deep cryogenic treatment on the microstructure and corrosion behavior of the microarc oxidized Mg-2 . 0Zn-0 . 5Ca alloy *Integr. Med. Res.* **9** 3943–9
[12] Peron M, Bertolini R, Ghiotti A, Torgersen J, Bruschi S and Berto F 2020 Journal of the mechanical behavior of biomedical materials enhancement of stress corrosion cracking of AZ31 magnesium alloy in simulated body fl uid thanks to cryogenic machining *J. Mech. Behav. Biomed. Mater.* **101** 103429
[13] Beura V K, Kale C, Srinivasan S, Williams C L and Solanki K N 2020 Corrosion behavior of a dynamically deformed Al-Mg alloy *Electrochim. Acta* **354** 136695
[14] Kirkland N T, Lespagnol J, Birbilis N and Staiger M P 2010 A survey of bio-corrosion rates of magnesium alloys *Corros. Sci.* **52** 287–91
[15] Lim M L C, Kelly R G and Scully J R 2016 Overview of intergranular corrosion mechanisms, phenomenological observations, and modeling of AA5083 *NACE International* 72 (*Corrosionscience: Intergranular corrosion*) pp 198–220
[16] McCafferty E 2003 Sequence of steps in the pitting of aluminum by chloride ions *Corros. Sci.* **45** 1421–38
[17] Trueba M and Trasatti S P 2010 Study of Al alloy corrosion in neutral NaCl by the pitting scan technique *Mater. Chem. Phys.* **121** 523–33
[18] Chao C Y, Lin L F and Macdonald D D 1981 A point defect model for anodic passive films: I . film growth kinetics *J. Electrochem. Soc.* **128** 1187–94

[19] Lin L F, Chao C Y and Macdonald D D 1981 A point defect model for anodic passive films: II . chemical breakdown and pit initiation *J. Electrochem. Soc.* **128** 1194–8
[20] Ramesh S, Bhuvaneshwari B, Palani G S, Lal D M, Mondal K and Kumar R 2019 Enhancing the corrosion resistance performance of structural steel via a novel deep cryogenic treatment process *Vacuum* **159** 468–75
[21] Paulin P 1993 Frozen Gears *Gear Technol.* **10** 26–9
[22] Steels V H 2021 Effect of deep cryogenic treatment on corrosion properties of various high-speed steels *Metals* **11** 1–16
[23] Syed Z F, Tamilarasan T R and Dennison M S 2021 Effect of novel cryogenic treatment in the corrosion behaviour , microstructure analysis and electrochemical properties of Al 6101 closed-cell foam *Aust. J. Mech. Eng.* 1–16 (In Press)
[24] Santosh R, Ahmed M, Lokesha M and Manjunath L H 2020 Investigating the impact of deep cryogenic treatment on surface roughness and cutting force in turning C45 steel *Mater. Today Proc.* **24** 1190–8
[25] Agrawal C, Wadhwa J, Pitroda A, Pruncu C I, Sarikaya M and Khanna N 2021 Comprehensive analysis of tool wear, tool life, surface roughness, costing and carbon emissions in turning Ti–6Al–4V titanium alloy: cryogenic versus wet machining *Tribol. Int.* **153** 106597
[26] Özbek N A, Çiçek A, Gülesin M and Özbek O 2014 Investigation of the effects of cryogenic treatment applied at different holding times to cemented carbide inserts on tool wear *Int. J. Mach. Tools Manuf* **86** 34–43
[27] Odewunmi N A, Solomon M M, Umoren S A and Ali S A 2020 Comparative studies of the corrosion inhibition efficacy of a dicationic monomer and its polymer against API X60 steel corrosion in simulated acidizing fluid under static and hydrodynamic conditions *ACS Omega* **5** 27057–71
[28] Abd El-Lateef H M 2020 Corrosion inhibition characteristics of a novel salycilidene isatin hydrazine sodium sulfonate on carbon steel in HCl and a synergistic nickel ions additive: a combined experimental and theoretical perspective *Appl. Surf. Sci.* **501**
[29] Farag A A and Ali T A 2015 The enhancing of 2-pyrazinecarboxamide inhibition effect on the acid corrosion of carbon steel in presence of iodide ions *J. Ind. Eng. Chem.* **21** 627–34
[30] Chevalier M, Robert F, Amusant N, Traisnel M, Roos C and Lebrini M 2014 Enhanced corrosion resistance of mild steel in 1 M hydrochloric acid solution by alkaloids extract from Aniba rosaeodora plant: electrochemical, phytochemical and XPS studies *Electrochim. Acta* **131** 96–105
[31] Majd M T, Ramezanzadeh M, Ramezanzadeh B and Bahlakeh G 2020 Production of an environmentally stable anti-corrosion film based on Esfand seed extract molecules-metal cations: integrated experimental and computer modeling approaches *J. Hazard. Mater.* **382** 121029
[32] Hu Q, Qiu Y, Zhang G and Guo X 2015 Capsella bursa-pastoris extract as an eco-friendly inhibitor on the corrosion of Q235 carbon steels in 1 mol·L- 1 hydrochloric acid *Chinese J. Chem. Eng.* **23** 1408–15
[33] Tang J, Luo H, Qi Y, Xu P, Ma S and Zhang Z 2018 The effect of cryogenic burnishing on the formation mechanism of corrosion product fi lm of Ti-6Al-4V titanium alloy in 0 . 9 % NaCl solution *Surf. Coat. Technol.* **345** 123–31
[34] Gerengi H, Sen N, Uygur I and Solomon M M M 2019 Corrosion response of ultra-high strength steels used for automotive applications *Mater. Res. Express* **6** 0865a6
[35] Solomon M M, Umoren S A, Obot I B, Sorour A A and Gerengi H 2018 Exploration of Dextran for application as corrosion inhibitor for steel in strong acid environment: effect of molecular weight, modification, and temperature on efficiency *ACS Appl. Mater. Interfaces* **10** 28112–29
[36] Amini K, Nategh S, Shafyei A and Rezaeian A 2010 The effect of deep cryogenic treatment on mechanical properties of 80CrMo12 5 tool steel *Int. J. ISSI* **7** 12–7
[37] Harish S, Bensely A, Mohan Lal D, Rajadurai A and Lenkey G B 2009 Microstructural study of cryogenically treated En 31 bearing steel *J. Mater. Process. Technol.* **209** 3351–7
[38] Kong L B, Huang Y, Que W, Zhang T, Li S, Zhang J, Dong Z and Tang D 2015 Ceramic Powder Synthesis *Topics in Mining, Metallurgy and Materials Engineering* (Berlin, Germany: Springer Science and Business Media Deutschland GmbH) pp 93–189
[39] Franco Steier V, Ashiuchi E S, Reißig L and Araújo J A 2016 Effect of a deep cryogenic treatment on wear and microstructure of a 6101 aluminum alloy *Adv. Mater. Sci. Eng.* **2016** 1–12